National Weather Association, *Electronic Journal of Operational Meteorology*, 2009-EJ4

Significant Nighttime Tornadoes in the Plains Associated with Relatively Stable Low-Level Conditions

Anthony Fischer
Aviation Weather Center, Kansas City, Missouri

Jonathan M. Davies
Private Meteorologist, Trimble/Kansas City, Missouri

(*Manuscript received* 13 January 2009; *In final form* 29 June 2009)

ABSTRACT

Nighttime cyclic tornadic supercells occurred in northern Kansas on both 29 May and 11 June of 2008, the latter event resulting in two fatalities. The supercells produced significant tornadoes within environments containing unusually large near-surface CIN. The synoptic scale and mesoscale evolution of each event is examined, with an emphasis on the thermodynamic and vertical shear characteristics of the near-storm environment. It is hypothesized that anomalously strong CAPE-shear combinations in each case contributed to the generation of long-lived supercells with intense vertical pressure gradients, allowing the storms to produce tornadoes in environments characterized by a deep stable near-surface layer.

1. Introduction

Although nighttime tornadoes are less common in the Plains than the deep South (e.g., Grazulis 1993), recent years have seen an atypically large number of nighttime events in the Plains. These include such deadly tornadoes as Holly, CO (EF-3) on 28 March 2007; Greensburg, KS (EF-5) on 4 May 2007; and Lone Grove, OK (EF-4) on 10 February 2009. The impact of these events on life and property underscores the importance of anticipating the threat of nighttime tornadoes for operational forecasters in the Plains.

A database study of Rapid Update Cycle (RUC, Benjamin et al. 2004) analysis soundings in Davies and Fischer (2009, hereafter DF09) examined nighttime supercell tornado environments in the eastern two-thirds of the United States. One of the findings was that

Corresponding author address: Anthony Fischer, Aviation Weather Center, 7220 NW 101st Terrace, Kansas City, MO 64153-2371
E-mail: Andy.Fischer@noaa.gov

nighttime significant tornadoes tend to occur in settings with relatively weak convective inhibition (CIN, Colby 1984), similar to overall results in Davies 2004. This is an atypical situation in the Plains states, because CIN often increases substantially with diurnal cooling after dark due to the high frequency of elevated mixed layers (EML, Carlson et al. 1983) originating over adjacent southwestern states. Large near-surface CIN acts to reduce tornado potential, as inflow air parcels must be lifted through a stable near-surface layer or are rooted above the layer. When *moderate to small* nighttime CIN occurs in the Plains (i.e., generally less than 50-75 J kg^{-1}), this suggests an environment that is supportive of surface-based convection—a beneficial factor for nighttime tornadoes when other characteristics such as sufficient convective available potential energy (CAPE) and storm-relative helicity (SRH, Davies-Jones et al. 1990) are present.

However, from time to time, significant nighttime tornadoes do occur with relatively large CIN in the Plains, where the near-storm environment does not appear as strongly surface-based as the DF09 results for nighttime strong/violent tornadoes would suggest. In 2008, significant tornadoes occurred after dark in northern Kansas on 29 May and 11 June (see **Table 1** and **Fig. 1**) in environments containing unusually large CIN for significant tornadoes. In these cases, the near-surface environment was atypically characterized by a rather deep stable layer, and was not strongly surface-based. Each of these events will be discussed, and common features and implications for forecasters will conclude the paper.

2. Analysis

Observed and numerical model data were examined to study the synoptic and mesoscale evolution of the 29 May and 11 June events. In particular, RUC model soundings were used to assess thermodynamic and vertical shear characteristics of each near-storm environment.

Though the RUC has been shown to reasonably approximate supercell environments (Thompson et al. 2003), surface observations, radiosonde observations (RAOBs), and wind profilers were also analyzed to gauge the representativeness of the RUC data and to modify soundings and hodographs accordingly. The virtual temperature correction (Doswell and Rasmussen 1994) was applied to thermodynamic computations, and lowest 100-hPa mixed-layer (ML) parcels were emphasized given their superior correlation to observed convective cloud base heights (Craven et al. 2002). Storm-relative shear parameters were computed using observed storm motions.

a. 29 May 2008: Jewell, KS and Belleville, KS area tornadoes

A broad upper level trough progressed from the western U.S. to the northern and central Plains on 29 May (**Fig. 2**). At the base of this trough, seasonably strong 500-hPa and 300-hPa jet streaks (30 and 50 m s^{-1} respectively) and modest mid-level height falls overspread the central Plains during the afternoon. At the surface, a dryline mixed into the central high Plains, bulging into southwestern Nebraska and northwestern Kansas (**Fig. 3**). Large scale forcing for ascent and divergent upper level flow aided convective initiation along this portion of the dryline by 1930 UTC. The large scale ascent would continue to support these storms, many of which evolved into supercells, as they moved eastward through the warm sector for the next several hours.

The storm of interest gradually evolved from the tail-end of this convection near the Kansas-Colorado border, acquiring supercell characteristics near Oakley, KS at 2200 UTC (refer to **Fig. 1**) and maintaining favorable inflow the next several hours. The storm was primarily nontornadic during its first three hours, producing only two brief EF-0 tornadoes near Zurich, KS at 0010 UTC. After 0100 UTC, the supercell became an efficient tornado producer, generating several EF-0 tornadoes between Osborne and Tipton, KS from 0118-0140 UTC. Then the storm

went on to produce two large, long-tracked EF-3 tornadoes near and after dark from 0140-0405 UTC (see **Table 1**), the first of which struck the community of Jewell, KS. The supercell was finally absorbed by a quasi-linear convective system over south-central Nebraska.

The environment in northwestern Kansas was supportive of supercells (Rasmussen and Blanchard 1998, hereafter RB98) by late afternoon on 29 May, with MLCAPE of 1500-2000 J kg^{-1} and 0-6 km bulk shear of 22-30 m s^{-1} (43-58 kt) per modified RUC soundings. Also, low-level shear was large as early as 2300 UTC (0-1 km SRH of 400 m^2 s^{-2}) due to a 20-25 m s^{-1} low-level jet (LLJ) present over the warm sector and strongly favorable storm-relative inflow. However, high lifting condensation level (LCL) heights resulting from deep mixing and modest boundary layer moisture were initially unfavorable for tornadogenesis (e.g., RB98), with surface temperatures in excess of 30°C (86°F) and dew points only near 15°C (59°F).

After 0000 UTC, a number of factors became increasingly favorable for tornadoes in the near-storm environment. LCL heights lowered as the boundary layer diurnally cooled and the storm moved fully into the rich moist axis (surface dew points of 19-21°C or 66-70°F), as in **Fig. 4**. Increasing boundary layer moisture likewise contributed to stronger instability. Meanwhile, wind profilers and surface observations indicated a notable increase in low-level shear over the area as the boundary layer began to decouple, resulting in weakening surface winds in far north-central Kansas and south-central Nebraska and nocturnal acceleration of the LLJ to 30 m s^{-1} (Bonner 1968). Surface winds also backed to southeasterly, possibly in response to strong vertical motion overspreading the warm sector, which further enlarged low-level hodographs.

However, a stable layer in the low levels was also increasing. Trajectories from the 0000 UTC 700-hPa RAOB plot (see **Fig. 5**) indicated a substantial EML spreading northeastward toward north-central Kansas from the southern high Plains. Upstream of the storm, Dodge City

RAOBs showed considerable 700-500-hPa warming during the day in association with the expanding EML (**Fig. 6**), with a 700-hPa temperature of 13.4°C at 0000 UTC—a probable reason storms were limited to the northern third of Kansas during the evening.

A modified 0300 UTC RUC analysis sounding at Belleville, KS (**Fig. 7**) was used to estimate the environment during the significant tornadic phase of the supercell. The RUC showed the richest boundary layer moisture to be unreasonably shallow; thus the moisture profile was modified based on interpolated mean mixing ratios within regional 00Z RAOBs. Steep lapse rates aloft resulted in strong instability, with MLCAPE of 2747 J kg^{-1}. MLLCL heights were also favorably low at 936 m. Still, diurnal cooling beneath the expanding elevated mixed layer resulted in a MLLFC (level of free convection) height near 3 km and MLCIN of 120 J kg^{-1}. Given the decoupled nature of the boundary layer with a weak near-surface temperature inversion per the modified sounding, it is likely the inflow air mass was no longer well mixed and that a ML lifted parcel would not be most appropriate for assessing the thermodynamic environment. Lifting a surface-based (SB) parcel resulted in even stronger inhibition given the surface inversion, with CIN of 211 J kg^{-1}; while lifting the most unstable (MU) parcel, which resided at 900-hPA just above the inversion, produced CIN of 108 J kg^{-1}. Visual characteristics of the storm's updraft during its significant tornadic phase (**Fig. 8**) were certainly suggestive of substantial inhibition, with stratiform laminar banding (rather than a cumuliform appearance) in the lowest few kilometers indicative of forced ascent through a stable layer.

Figure 9 shows the corresponding modified 0300 UTC RUC analysis hodograph at Belleville. The RUC surface wind was slightly too strong and veered to be representative per surface observations; thus, the mean surface wind at Concordia, KS from 0130-0300 UTC was substituted. Deep layer shear was strongly supportive of supercells, with 0-6 km bulk shear of

31 m s^{-1} (60 kt). Meanwhile, very strong speed shear was present in the near-surface layer, with southeasterly surface flow near 5 m s^{-1} and southerly 500 m AGL flow of 28 m s^{-1}. Accordingly, despite the storm motion having curved markedly to the left (from 255° to 232°) just prior to its significant tornadic phase, unseasonably large low-level shear was available with 0-1 km SRH of 661 m^2 s^{-2}. The combination of strong instability and very strong low-level shear resulted in anomalously large energy-helicity indices (EHI, Hart and Korotky 1991; Davies 1993), with a 0-1 km EHI of 11.3 based on the modified sounding and hodograph.

b. 11 June 2008: tornadoes at Salina, Chapman, Manhattan, and Soldier, KS

A large, unseasonably deep upper level trough moved from the northwestern U.S. toward the northern and central Plains on 11 June (see **Fig. 10**). A cold front served as the focus of convective initiation, with quasi-linear severe storms developing from southwestern Minnesota to eastern Nebraska during 2100-2300 UTC as strengthening mid-level flow and large scale ascent interacted with the front. Explosive initiation concurrently took place across central and north-central Kansas (see **Fig. 11**) near the northern edge of a capping EML that had encompassed the southern Plains (**Fig. 12**). Several training supercells resulted here, with deep layer shear vectors oriented west-to-east resulting in a sufficiently large angle with the cold front for discrete mode (e.g., Dial and Racy 2004). Unseasonably strong mid-level flow of 30-40 m s^{-1} aided in the eastward propagation of these supercells off the boundary.

The supercell of interest initiated northwest of Great Bend, KS about 0030 UTC and quickly attained supercell characteristics as it moved rapidly eastward (refer to **Fig. 1**). By 0210 UTC the storm was producing hail to the size of softballs (11 cm in diameter). The storm then became tornadic after dark, intermittently producing four significant tornadoes between 0240 and

0511 UTC (see **Table 1**). Two of these tornadoes caused one fatality each in Chapman, KS and near Soldier, KS; while another affected Manhattan, KS, including the Kansas State campus.

Per modified RAOBs and wind profilers, an impressive combination of instability (MLCAPE near 2500 J kg^{-1}) and deep layer shear (0-6 km bulk shear in excess of 30 m s^{-1} or 58 kt) was initially present in the storm's environment. Low-level shear was also quite large as the storm moved through the nose of the 25-30 m s^{-1} LLJ immediately ahead of the cold front; 0-1 km SRH was initially around 350 m^2 s^{-2}, and gradually strengthened with time as the storm tracked into lighter and more backed surface winds present in the richest moist axis just east of the I-135 corridor. Although LCL heights were at first marginally high for a significant tornado threat with surface temperatures and dew points near 30°C and 18°C (86°F and 64°F), the storm propagated quickly into the moist axis near I-135 as surface temperatures cooled diurnally.

However, as with the 29 May case, convective inhibition became considerable after dark due to the magnitude of the warm air aloft. **Figure 13** shows an overlay of the 1800 and 0000 UTC Topeka RAOBs just downstream of the storm, which sampled the northern fringe of the expanding EML and a 700-hPa temperature of 12.8°C by 0000 UTC. In the near-storm environment, RUC model trends indicated neutral temperature advection within the capping layer between 0100-0400 UTC, and substantial cooling of the layer thereafter as the leading edge of cold air advection aloft was forecast to rapidly overspread northeastern Kansas.

A modified 0300 UTC RUC analysis sounding at Chapman, KS (**Fig. 14**) was used to approximate the near-storm environment during the first three significant tornadoes, when MLCIN for near-surface parcels was considerable (> 100 J kg^{-1}). The sounding indicated rich boundary layer moisture that appeared a bit too shallow and had cooled the boundary layer too quickly; thus, minor low-level modifications were made to the sounding based on regional

RAOBs and surface observations. Potential instability, though tempered by relatively warm air in the upper troposphere, was favorably strong with MLCAPE of 2004 J kg^{-1}. MLLCL heights of 1106 m were sufficiently low for significant tornadoes. Meanwhile, though the near-surface layer remained rather warm (surface temperatures near 27°C or 81°F through 0400 UTC), the EML maintained strong inhibition with MLLFC heights again near 3 km and MLCIN of 114 J kg^{-1}. Comparatively, lifting a surface-based parcel—which was also equivalent to the most unstable parcel—produced CIN of 100 J kg^{-1}. Given that the boundary layer likely remained fairly well mixed, lifting a ML parcel may have been reasonably appropriate for this case.

Figure 15 shows the corresponding modified RUC analysis hodograph for the storm. Because wind profilers indicated stronger middle and upper level flow than was initialized by the RUC, the 0300 UTC Hillsboro, KS wind profiler data was substituted above 4 km. Given the unseasonably strong mid-level jet, deep layer shear was very strong with 0-6 km bulk shear of 36.6 m s^{-1} (71 kt). Very large low-level shear was also present given strong speed shear and highly favorable storm-relative inflow, with 0-1 km SRH of 524 m^2 s^{-2}. The combination of moderate instability and very strong low-level shear contributed to very large EHI values (0-1 km EHI of 6.6), though not as anomalously large as in the 29 May case.

3. Results and Conclusion

These two events present a similar forecast challenge. Each resulted in significant damaging tornadoes after dark within environments of unusually large near-surface CIN. It was established that in each case, the strong CIN resulted from diurnal cooling beneath an EML accompanying the southeastern flank of the upper level trough. **Table 2** summarizes both events' thermodynamic and vertical shear parameters.

It is hypothesized that strong CAPE-shear combinations played a major role in allowing these storms to produce strong tornadoes within low-level air masses containing a significant stable layer. Each case possessed very strong low-level shear due to large, clockwise-curved hodographs associated with a nocturnally enhanced, significant (30 m s^{-1}) LLJ. Additionally, the storms occurred in environments with strong to very strong deep layer shear. The degree of vertical shear amidst strong potential instability likely contributed to intense vertical pressure perturbations (Rotunno and Klemp 1982) in the well-established supercells, acting to augment updraft strength and aid in tilting and stretching of horizontal vorticity through the stable layer.

The nighttime supercell RUC sounding database study in DF09 further puts these events into perspective. **Fig. 16** shows box and whisker plots of MLCIN from that study for daytime and nighttime subsets of non-tornadic, weak tornadic, and significant tornadic supercells. CIN appeared to discriminate rather well between nontornadic and significant tornadic supercells at night, and 90% of nighttime significant tornado cases occurred with less than 75 J kg^{-1} MLCIN. Though CIN was generally found to be larger with nighttime significant tornadoes in the Plains than those in the deep South, the 29 May and 11 June cases in this paper are still a considerable exception to the DF09 results. The MLCIN values from these cases (near 120 J kg^{-1}) fall well above the 90th percentile in the nighttime significant tornado category (**Fig. 16b**).

Figure 17 shows box and whisker plots of 0-1 km SRH in the DF09 database. The SRH values were by far largest for nighttime significant tornadoes; yet SRH on 29 May and 11 June was stronger than the vast majority of events in that category (**Fig. 17b**), with extreme values in the 525-660 m^2 s^{-2} range—further emphasizing the impressive nature of low-level shear in these cases. The database also showed most nighttime significant tornadoes in the Plains occur with much stronger instability than those in the deep South, and MLCAPE values in the 29 May and

11 June events (2000-2700 J kg^{-1}) are consistent with those results. Accordingly, 0-1 km EHI values were also very large on 29 May and 11 June (11.3 and 6.6, respectively), well above the 90th percentile for both daytime and nighttime significant tornadoes in the DF09 database (see **Fig. 18**). The potent CAPE-SRH combinations, coupled with strong deep layer shear, were probably a key factor that contributed to tornadogenesis processes which likely overcame the presence of large CIN.

These events should prompt forecasters to carefully monitor observed and model data in order to anticipate the nocturnal evolution of vertical shear in conjunction with that of potential instability and convective inhibition. Wind profilers and Velocity Azimuth Display (VAD) winds are useful in monitoring shear—particularly the LLJ magnitude, which contributes significantly to enhanced SRH after dark and is not always well forecast by short-term models. Representative surface wind vectors and parent storm motions should also be considered when assessing low-level shear in the near-storm environment, as both are critical to computing representative SRH and are likewise not always forecast well by models. Forecasters are urged to develop an awareness of potent CAPE-shear environments, such as the ones reviewed in this paper, which can contribute to dynamic pressure perturbations within supercells—enhancing nighttime tornado potential in spite of substantial near-surface inhibition in the Plains.

Finally, RUC model data should be used with caution when attempting to assess the magnitude of environmental CIN. Past experience indicates the RUC sometimes forecasts unrealistically shallow boundary layer moisture—as in the 29 May event—which can result in an overforecast of CIN. As with any event, interrogating RUC soundings alongside those from other models, in conjunction with RAOB and wind profiler/VAD wind data, can help forecasters gain confidence in the character and magnitude of low-level moisture and related CIN.

*Acknowledgements***.** The authors thank Bruce Entwistle for obtaining observed and model data for the two cases. The authors also thank Dr. Matthew Bunkers for providing a 250-m version of his hodograph spreadsheet, available at http://www.crh.noaa.gov/unr/?n=scm.

REFERENCES

Benjamin, S. G., and Coauthors, 2004: An hourly assimilation/forecast cycle: The RUC. *Mon. Wea. Rev.*, **132**, 495-518.

Bonner, W. D., 1968: Climatology of the low level jet. *Mon. Wea. Rev.*, **96**, 833-849.

Carlson, T. N., S. G. Benjamin, and G. S. Forbes, 1983: Elevated mixed layers in the regional severe storms environment: Conceptual model and case studies. *Mon. Wea. Rev.*, **111**, 1453-1473.

Colby, F. P., 1984: Convective inhibition as a predictor of convection during AVE-SESAME-2. *Mon. Wea. Rev.*, **112**, 2239-2252.

Craven, J. P., R. E. Jewell, and H. E. Brooks, 2002: Comparison between observed convective cloud-base heights and lifting condensation levels for two different lifting parcels. *Wea. Forecasting*, **17**, 885-890.

Davies, J. M., 2004: Estimations of CIN and LFC associated with tornadic and nontornadic supercells. *Wea. Forecasting*, **19**, 714-726.

-------, 1993: Hourly helicity, instability, and EHI in forecasting supercell tornadoes. Preprints, *17th Conf. on Severe Local Storms*, St. Louis, MO, Amer. Meteor. Soc., 107-111.

------- and A. Fischer, 2009: Environmental characteristics associated with nighttime tornadoes. *NWA Electronic Journal of Operational Meteorology*, 2009-EJ3.

Davies-Jones, R. P., D. Burgess, and M. Foster, 1990: Test of helicity as a tornado forecast parameter. Preprints, *16th Conf. on Severe Local Storms*, Kananaskis Park, AB, Canada, Amer. Meteor. Soc., 588-592.

Dial, G. L., and J. P. Racy, 2004: Forecasting short term convective mode and evolution for severe storms initiated along synoptic boundaries. Preprints, 22nd Conf. on Severe Local Storms, Hyannis, MA, Amer. Meteor. Soc., CD-ROM, 11A.2.

Doswell, C. A. III, and E. N. Rasmussen, 1994: The effect of neglecting the virtual temperature correction on CAPE calculations. *Wea. Forecasting*, **9**, 625-629.

Grazulis, T.P., 1993: *Significant Tornadoes, 1680-1991*. Environmental Films, St. Johnsbury, VT, 1326 pp.

Hart, J. A., and W. Korotky, 1991: The SHARP workstation v1.50 users guide. NOAA/National Weather Service. 30 pp. [Available from NWS Eastern Region Headquarters, 630 Johnson Ave., Bohemia, NY 11716.]

Rasmussen, E. N., and D. O. Blanchard, 1998: A baseline climatology of sounding-derived supercell and tornado forecast parameters. *Wea. Forecasting*, **13**, 1148-1164.

Rotunno, R. and J. B. Klemp, 1982: The influence of the shear-induced pressure gradient on thunderstorm motion. *Mon. Wea. Rev.*, **110**, 136-151.

Thompson, R. L., R. Edwards, J. A. Hart, K. L. Elmore, and P. M. Markowski, 2003: Close proximity soundings within supercell environments obtained from the Rapid Update Cycle. *Wea. Forecasting*, **18**, 1243-1261.

TABLES AND FIGURES

Table 1. Summary of significant tornadoes produced by nighttime cyclic tornadic supercells of 29 May and 11 June as described in study: Calendar date; begin/end time; begin/end location relative to cities; Enhanced Fujita scale rating; path length (PL); maximum path width (PW); fatalities (Fat); and injuries (Inj).

Date	Time	Location	Rating	PL	PW	Fat	Inj
05/29/08	0140-0214 UTC	3 km SSW Glen Elder KS – 3 km NNE Jewell KS	EF-3	31 km	1800 m	0	0
05/29/08	0230-0405 UTC	8 km SSE Formosa KS - 3 km NNW Jansen NE	EF-3	89 km	1200 m	0	0
06/11/08	0240-0257 UTC	6 km SSW Salina KS - 8 km ESE New Cambria KS	EF-3	26 km	200 m	0	0
06/11/08	0312-0337 UTC	2 km SE Enterprise KS - 10 km WSW Junction City KS	EF-3	24 km	800 m	1	3
06/11/08	0348-0403 UTC	2 km NNE Ogden KS – 2 km N Manhattan KS	EF-4	14 km	400 m	0	0
06/11/08	0446-0511 UTC	6 km ESE Onaga KS - 3 km SE Bancroft KS	EF-2	27 km	275 m	1	0

Table 2. Selected thermodynamic and vertical shear parameters in modified 0300 UTC RUC proximity sounding/hodograph for each the 29 May and 11 June tornado events.

	05/29/08	**06/11/08**
Sfc T/Td	24/20.5°C	27/20°C
700-hPa T	13.2°C	12.5°C
MLCAPE	2730 J kg^{-1}	2004 J kg^{-1}
MLLCL	936 m	1106 m
MLLFC	2934 m	2936 m
MLCIN	120 J kg^{-1}	114 J kg^{-1}
SBCIN	211 J kg^{-1}	100 J kg^{-1}
MUCIN	108 J kg^{-1}	100 J kg^{-1}
0-1 km SRH	661 m^2 s^{-2}	524 m^2 s^{-2}
0-1 km bulk shear	28.4 m s^{-1}	21.3 m s^{-1}
0-6 km bulk shear	31.2 m s^{-1}	36.6 m s^{-1}
0-1 km MLEHI	11.3	6.6

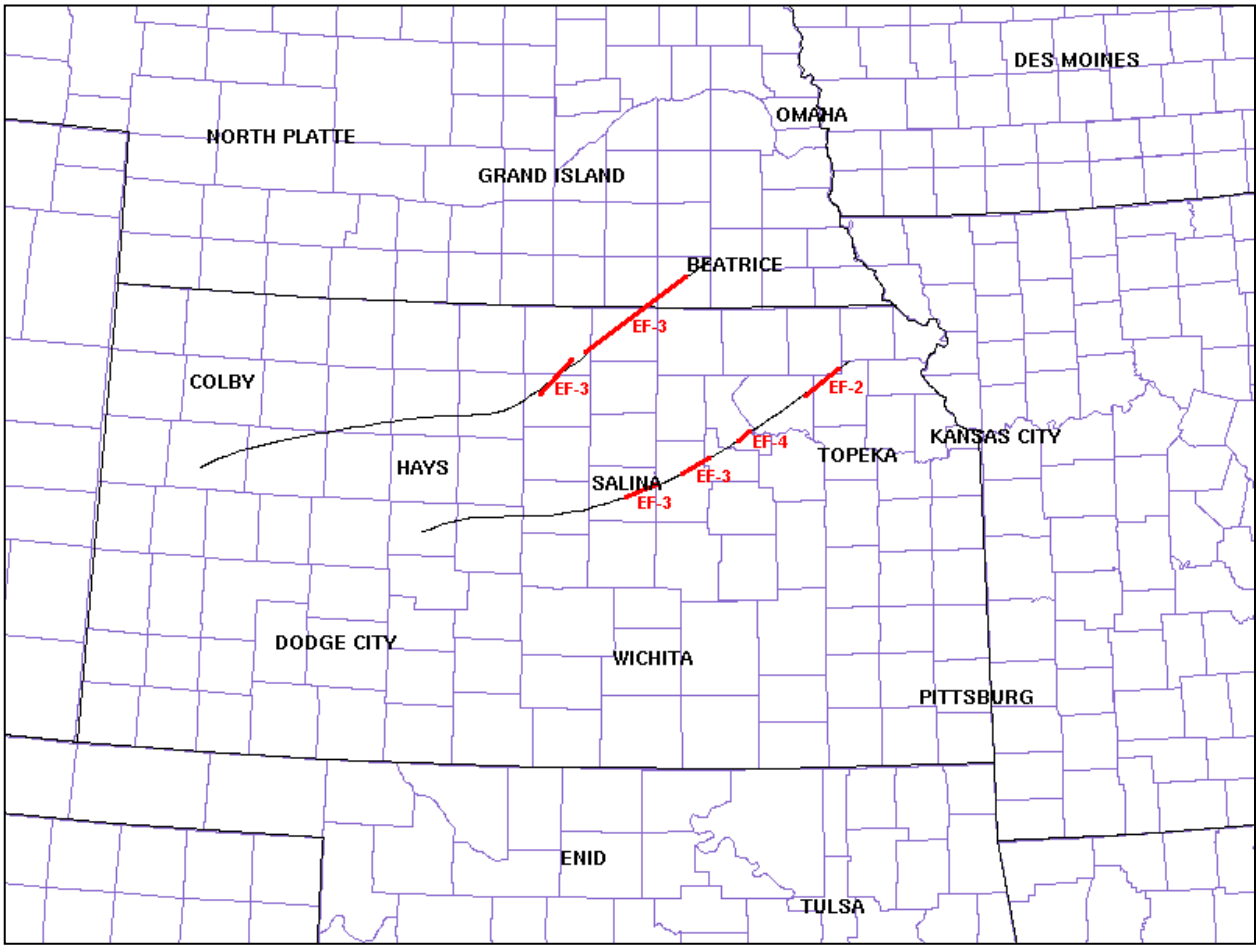

Figure 1. Map showing paths of 29 May (northwestern) and 11 June (southeastern) 2008 cyclic tornadic supercells in study. Mean paths of supercells denoted by thin black lines. Mean paths of significant tornadoes depicted by heavy red lines with attendant EF-scale ratings.

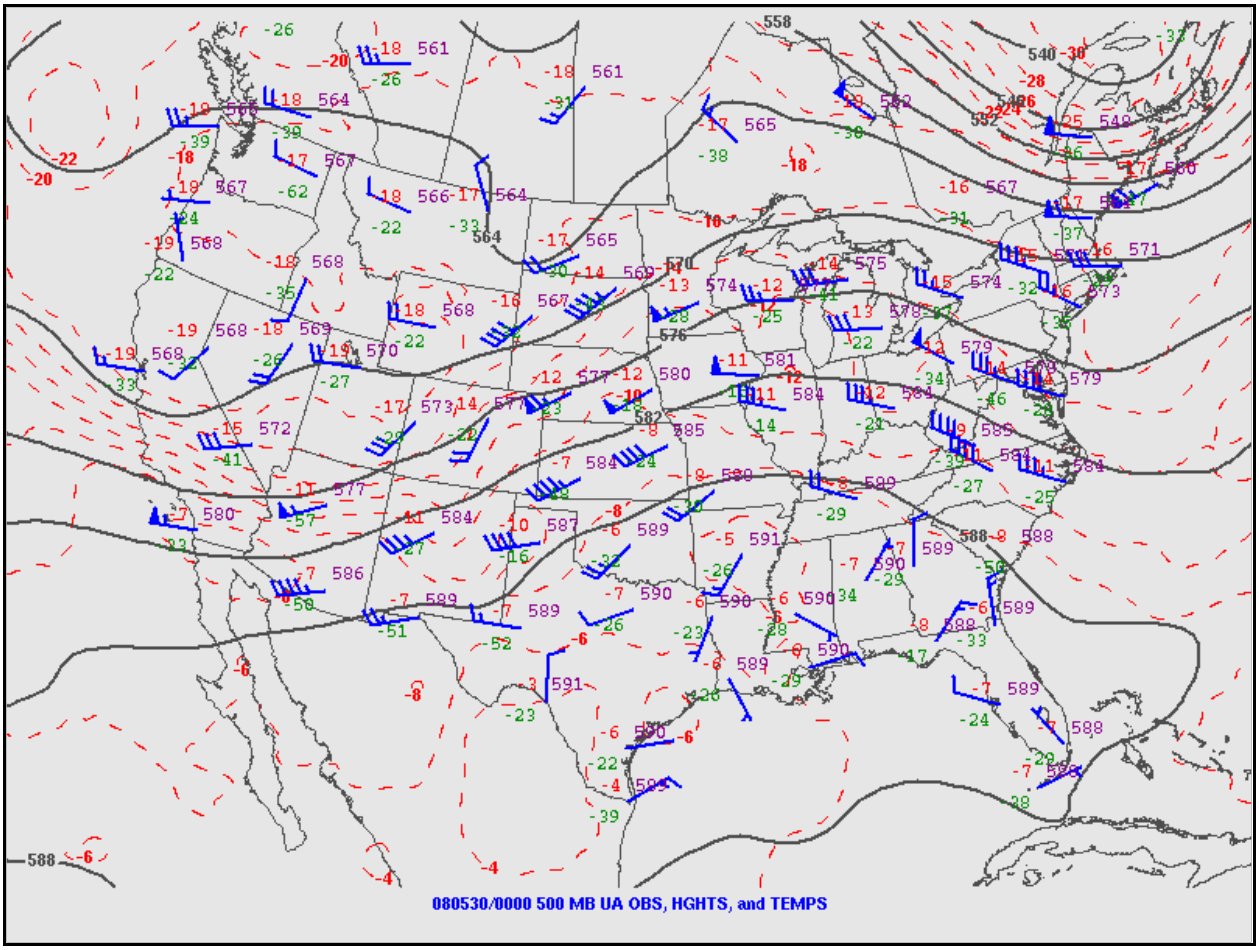

Figure 2. 0000 UTC 30 May 2008 500-hPa RAOB plot from Storm Prediction Center (SPC). 1800 UTC 29 May 2008 6-hour NAM-WRF forecast of temperature and geopotential height is overlaid as a first-guess initialization.

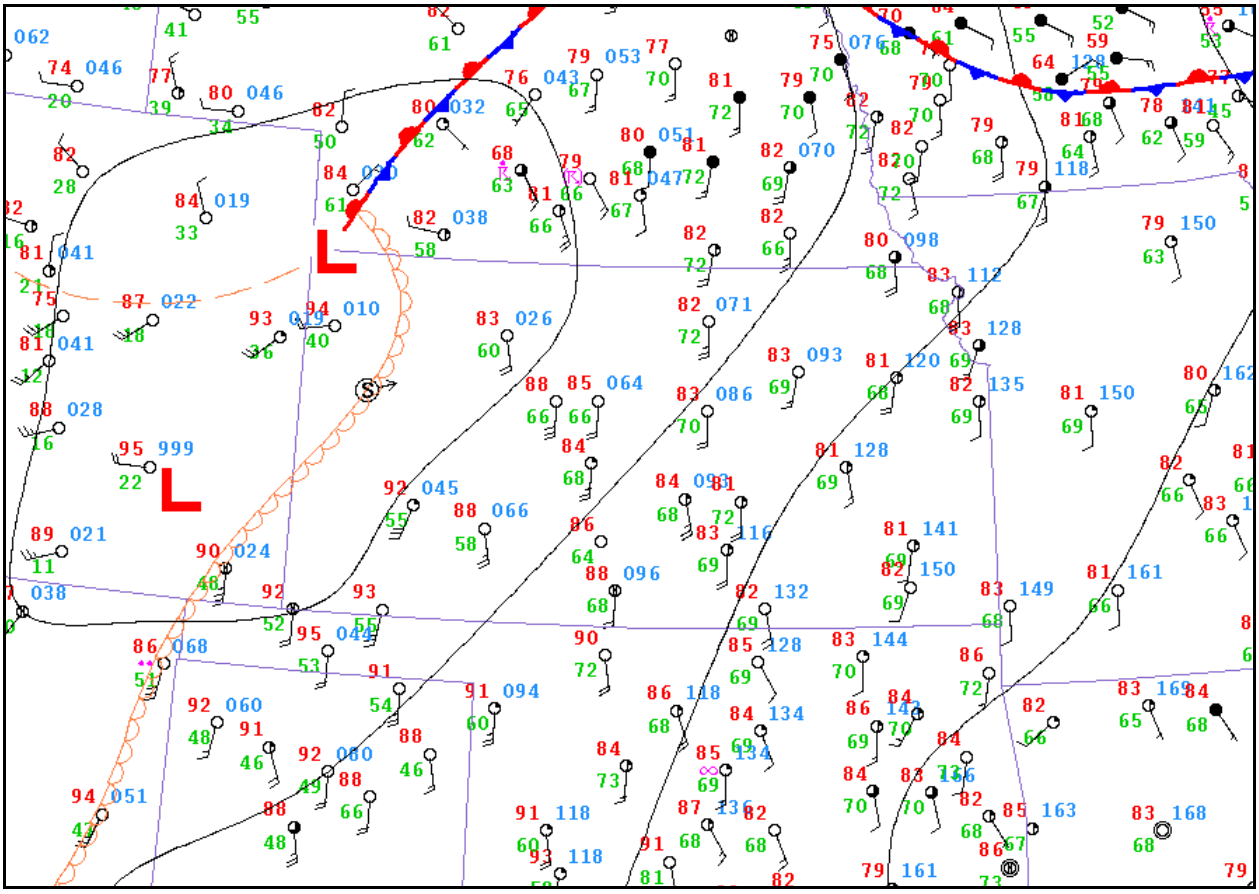

Figure 3. 2200 UTC 29 May 2008 surface observations over central Plains. Subjective surface analysis denoted with conventional symbols, and subjective mean sea level pressure contours analyzed every 4 mb. Position of developing supercell of interest denoted by circled "S" with movement arrow.

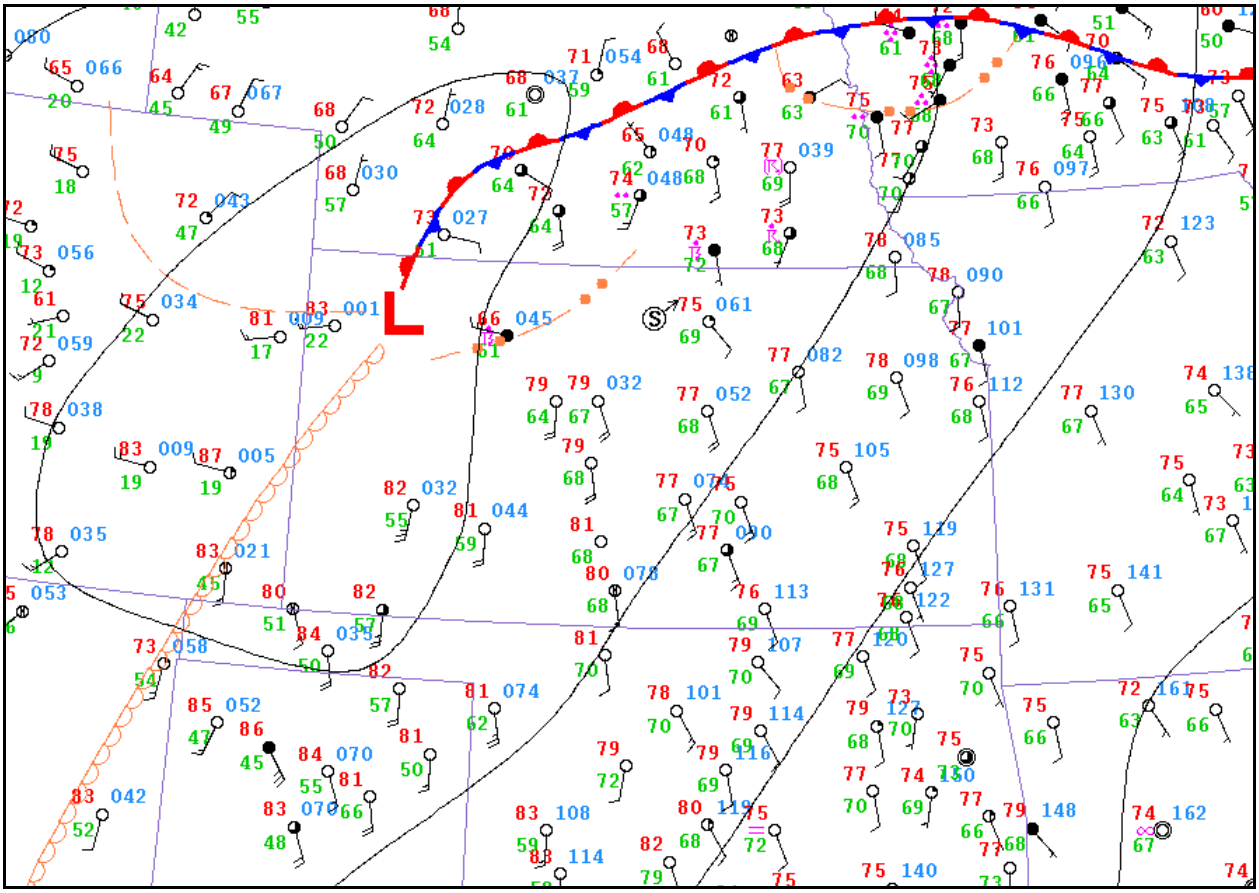

Figure 4. 0200 UTC 30 May 2008 surface observations and subjective analyses over central Plains, similar to Fig. 3. Position of supercell denoted by circled "S" with movement arrow.

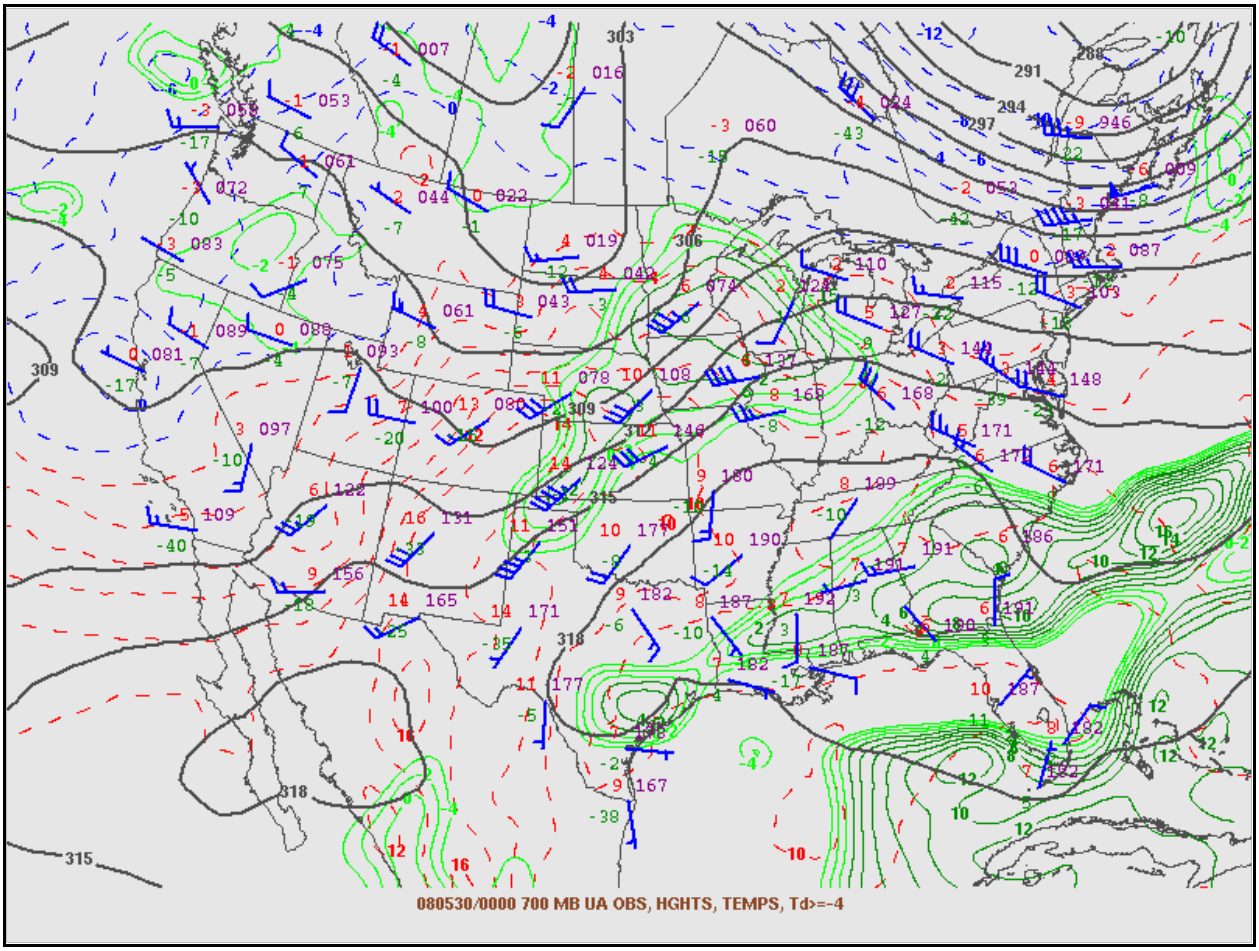

Figure 5. 0000 UTC 30 May 2008 700-hPa RAOB plot from SPC with NAM-WRF initialization as in Fig. 2.

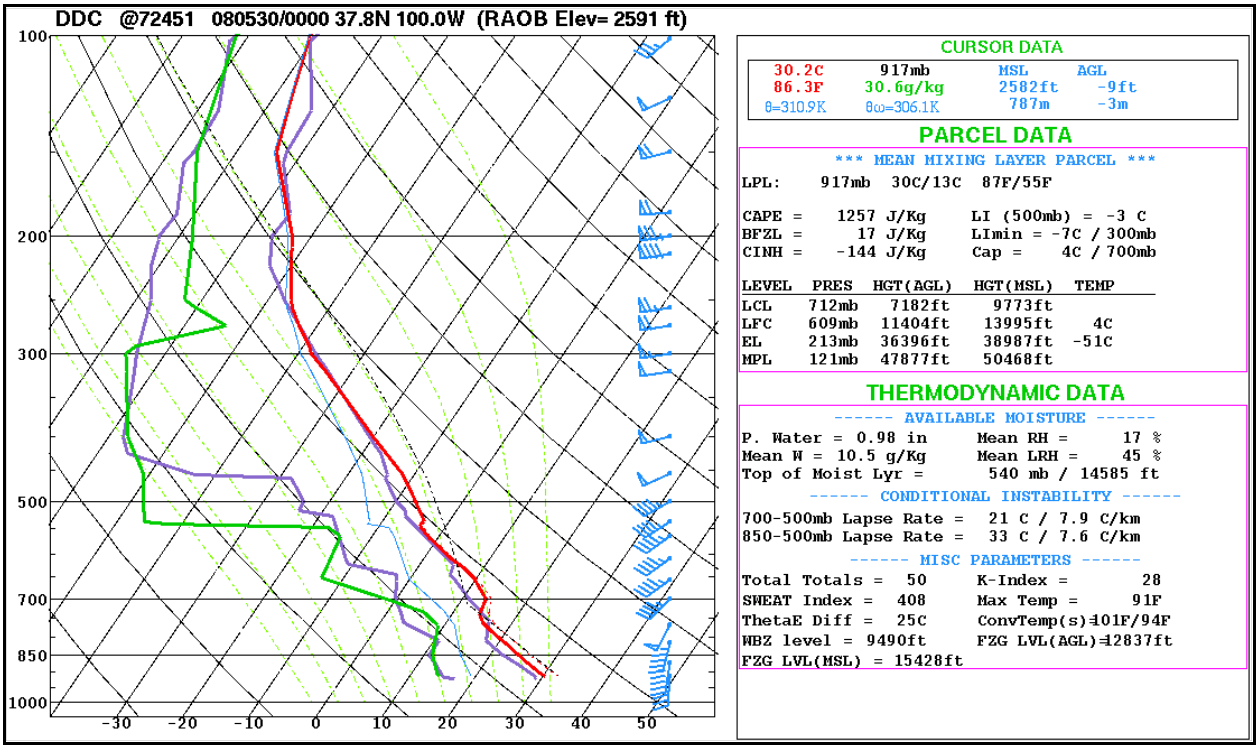

Figure 6. Overlay of 1800 UTC 29 May 2008 and 0000 UTC 30 May 2008 Dodge City, KS RAOBs in Skew*T*-log*p* format within NSHARP (Hart and Korotky 1991). 1800 UTC sounding depicted by purple temperature and dew point profile. Remaining temperature (red), virtual temperature (dashed red), dew point (green), ML lifted parcel trace (dashed black), and wind profile (blue)—and associated parameter computations—are from 0000 UTC sounding.

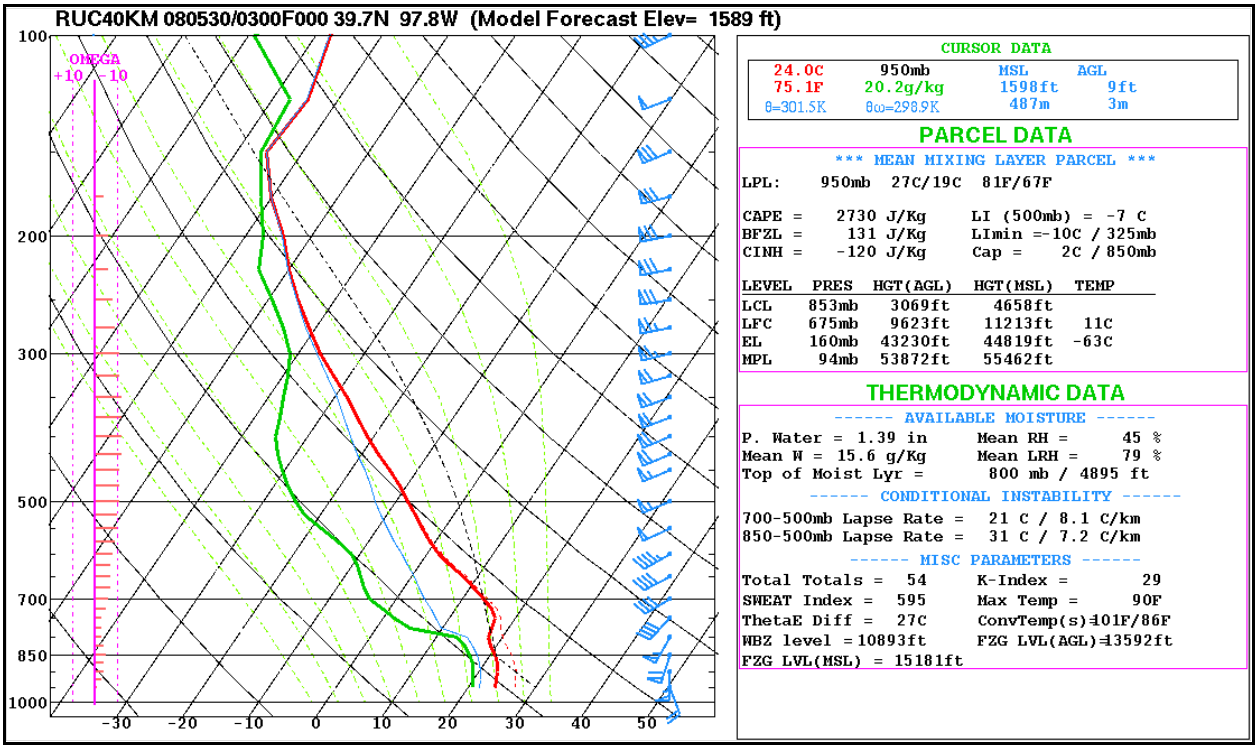

Figure 7. 0300 UTC 30 May 2008 modified RUC analysis sounding at Belleville, KS.

Figure 8. Panoramic photograph of the 29 May 2008 tornadic supercell at 0145 UTC, looking west from roughly 10 km east of Glen Elder, KS. The first of two significant tornadoes from the storm had touched down 5 minutes prior, ongoing in the photograph in an indistinct multiple vortex phase just to the left of the highway. Photograph is copyrighted by Matthew Ziebell.

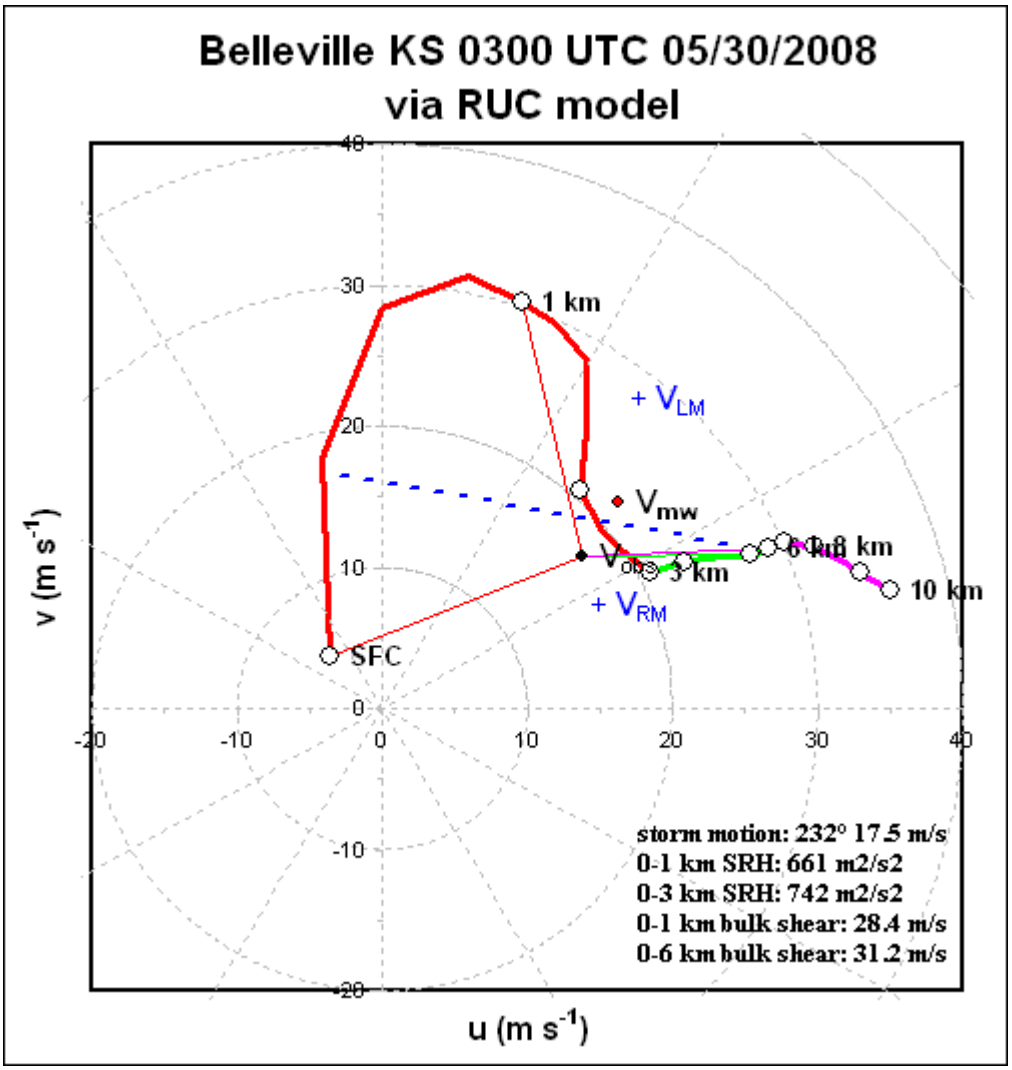

Figure 9. 0300 UTC modified RUC model 0-10 km hodograph at Belleville, KS, with data linearly interpolated to 250-m vertical increments. Mean surface wind observed at Concordia, KS substituted in spreadsheet. Observed storm motion denoted by V_{obs}. 0-1 km SRH bounded by surface and 1 km storm-relative wind vectors (thin red lines). Vertical shear parameters displayed in lower right corner.

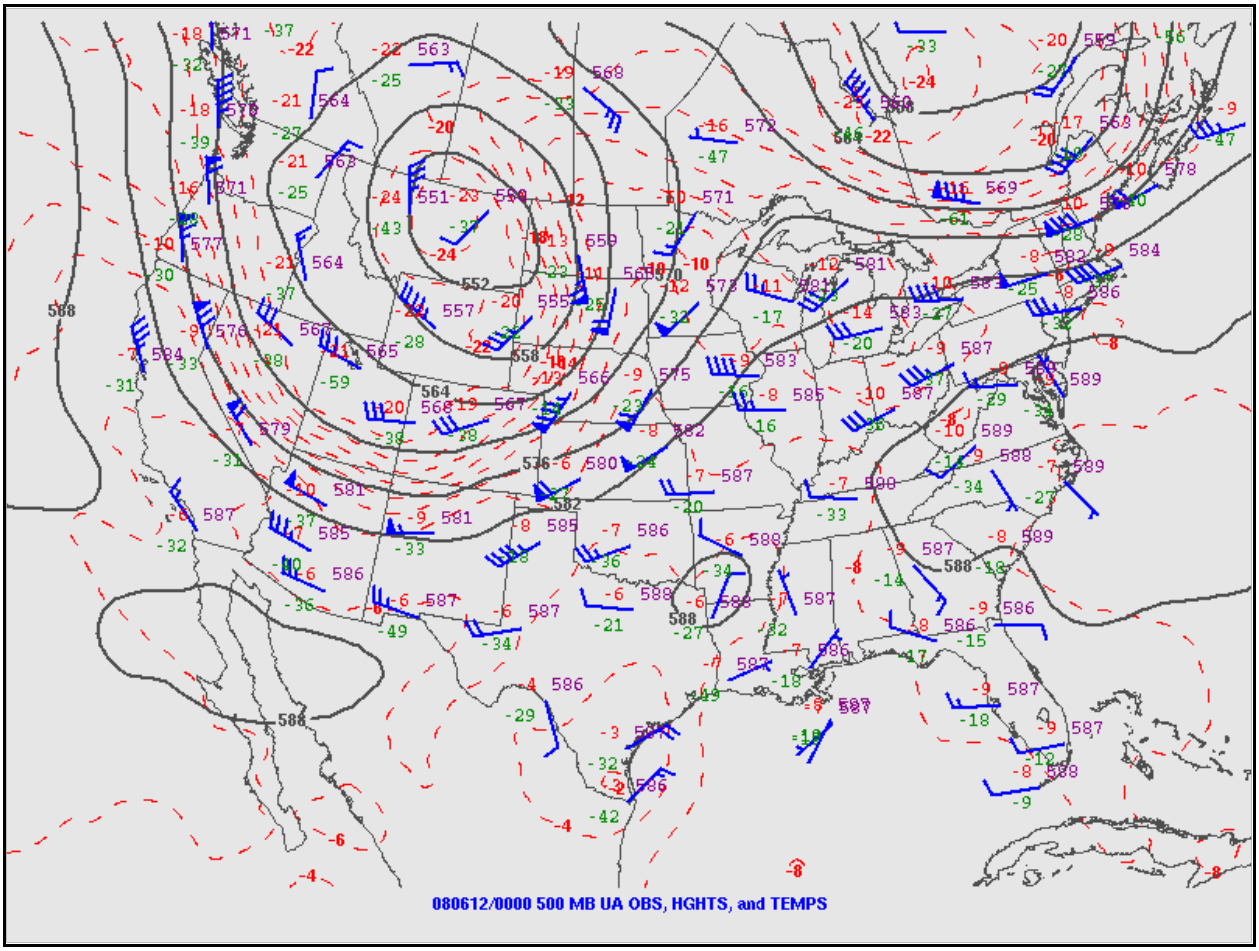

Figure 10. 0000 UTC 12 June 2008 500-hPa RAOB plot from SPC with NAM-WRF initialization as in Fig. 2.

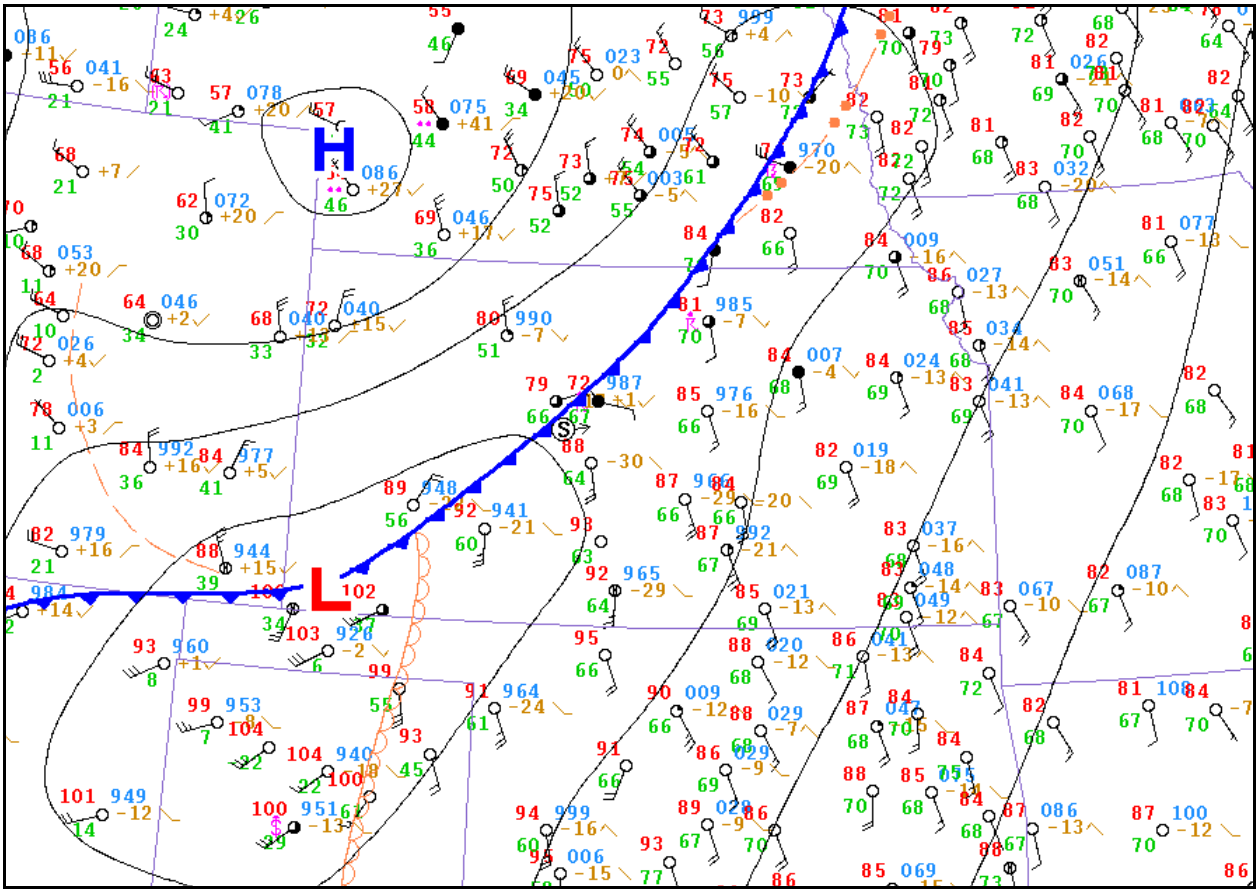

Figure 11. 0000 UTC 12 June 2008 surface observations and subjective analyses over central Plains, similar to Fig. 3. Position of developing supercell of interest denoted by circled "S" with movement arrow.

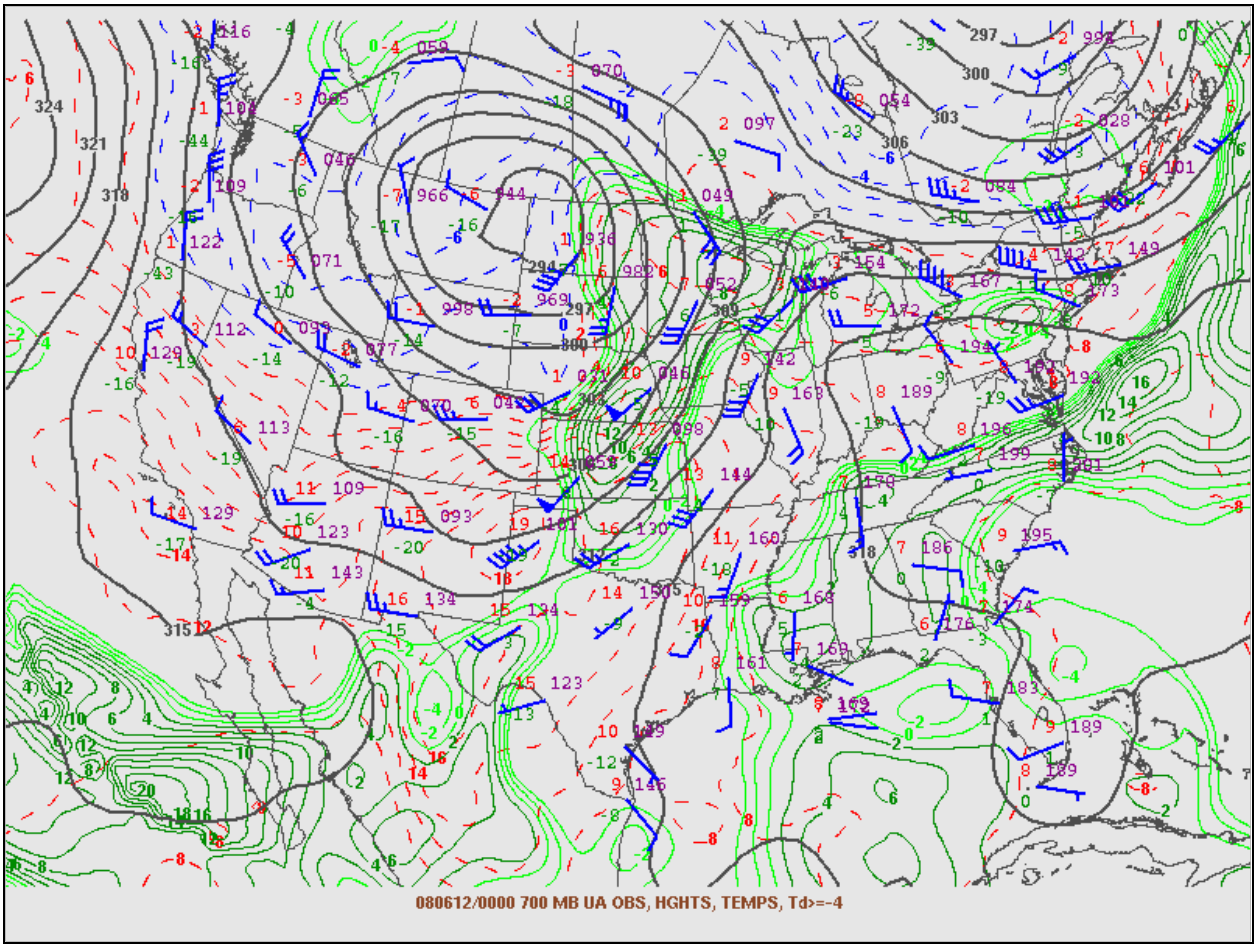

Figure 12. 0000 UTC 12 June 2008 700-hPa RAOB plot from SPC with NAM-WRF initialization as in Fig. 2.

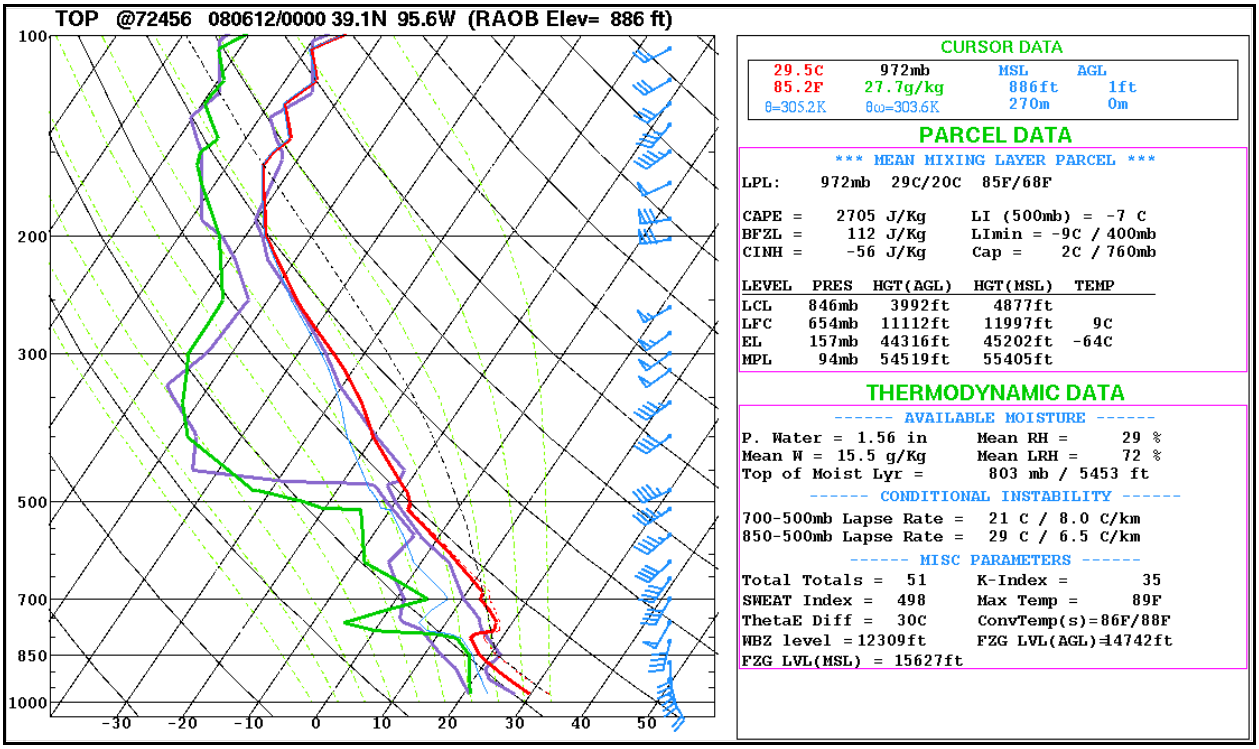

Figure 13. Overlay of 1800 UTC 11 June 2008 (purple temperature and dew point profile) and 0000 UTC 12 June 2008 Topeka, KS RAOBs, similar to Fig. 6.

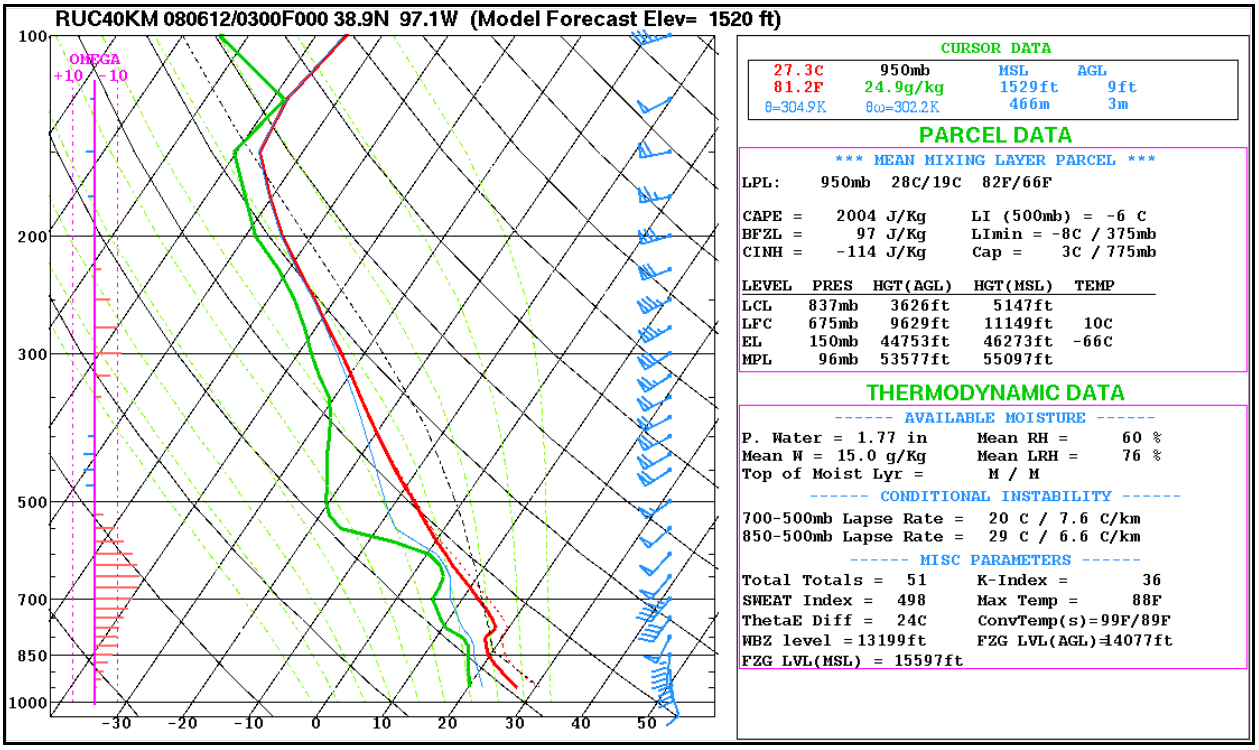

Figure 14. 0300 UTC 12 June 2008 modified RUC analysis sounding at Chapman, KS.

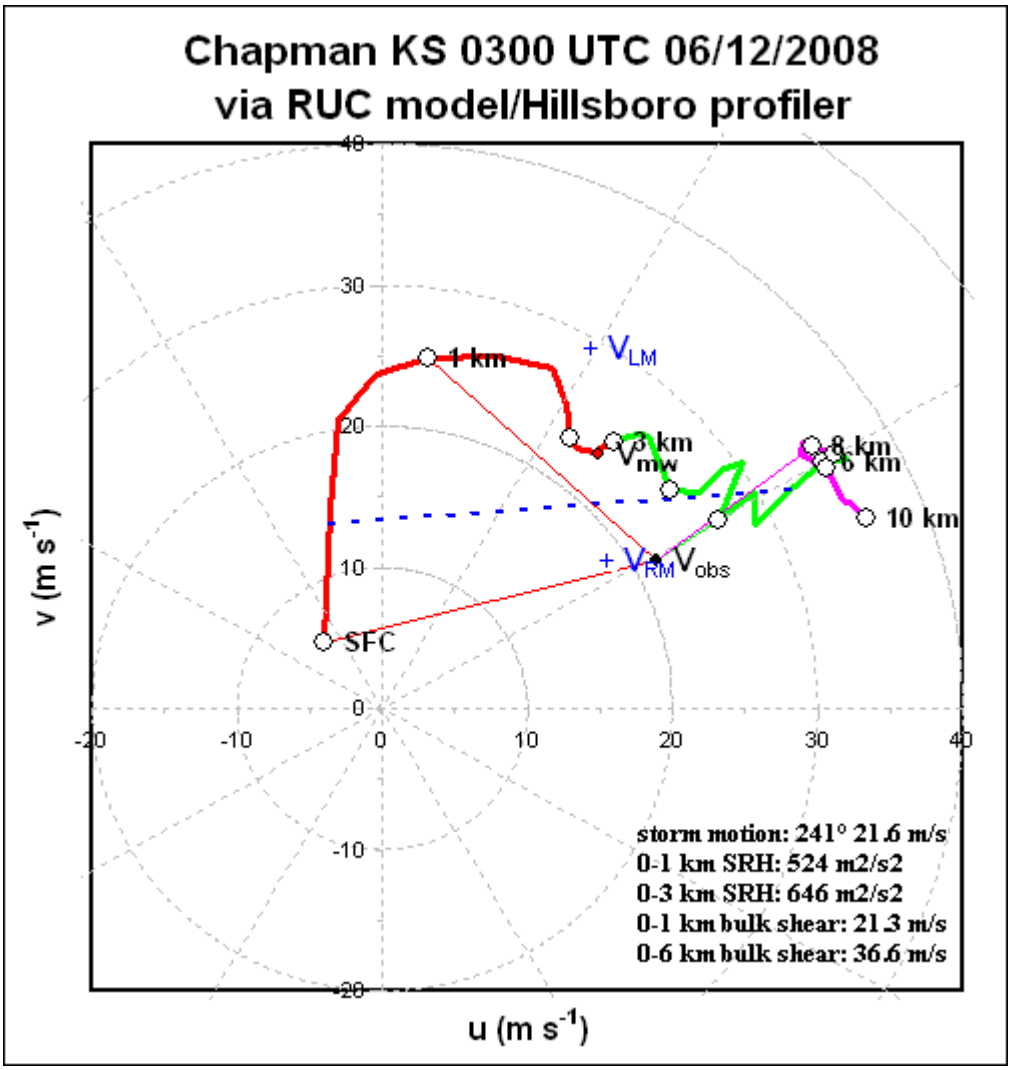

Figure 15. 0300 UTC 12 June 2008 modified RUC model 0-10 km hodograph at Chapman, KS, as in Fig. 8. 0300 UTC Hillsboro, KS wind profiler data substituted in 4-10 km layer.

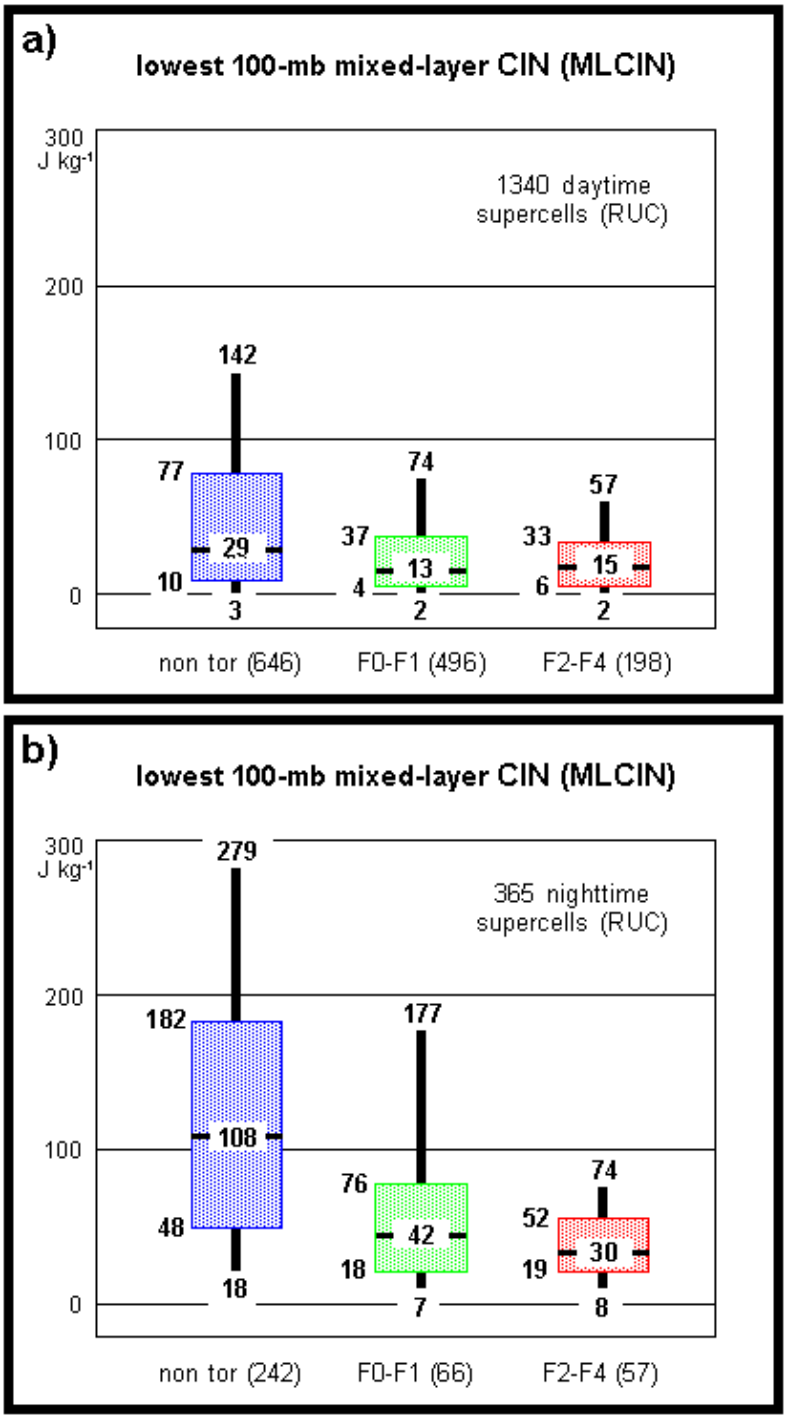

Figure 16. Box and whisker plots of MLCIN (J kg^{-1}) using lowest 100-mb mixed-layer lifted parcels for profiles in the DF09 database; (a) shows distributions for daytime supercells, and (b) nighttime supercells. Data are grouped as cases with no tornadoes ("non tor"; blue at left), weak tornadoes ("F0-F1"; green in middle), and significant tornadoes ("F2-F4"; red at right). Numbers in parentheses give total cases in each category. Boxes denote 25th to 75th percentiles, with horizontal bar showing median value. Whiskers extend to the 10th and 90th percentiles.

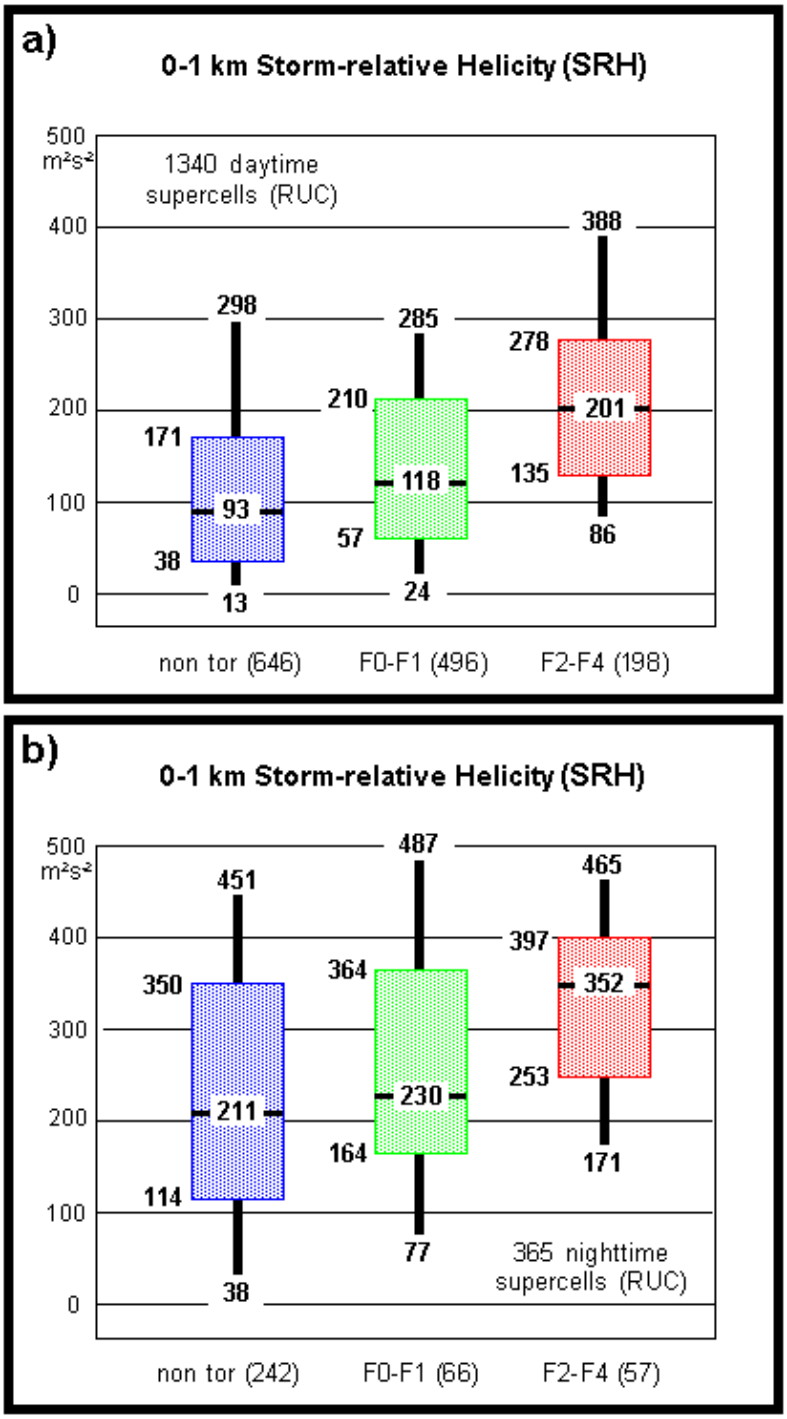

Figure 17. Box and whisker plots of 0-1 km SRH (m^2 s^{-2}) for profiles in the DF09 database, similar to Fig. 15.

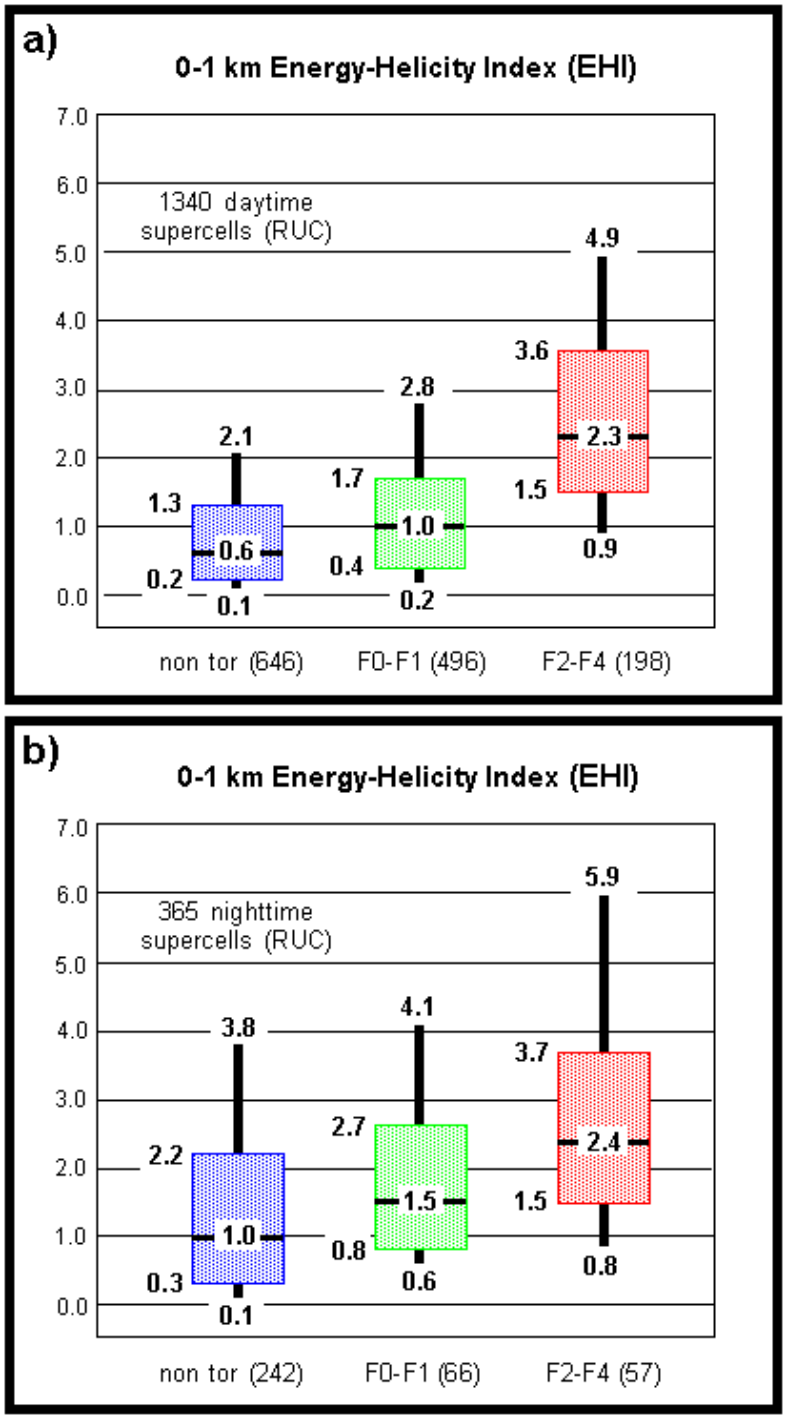

Figure 18. Box and whisker plots of 0-1 km EHI for profiles in the DF09 database, similar to Fig. 15.